Lightweight Distance and Relative Radial Velocity Estimation with a Passive RF Receiver

Milán Székely[1]

Supervisors: Arash Asadi[1]**, Florian Kosterhon**[1]

[1]**EEMCS, Delft University of Technology, The Netherlands**

A Thesis Submitted to EEMCS Faculty Delft University of Technology,
In Partial Fulfilment of the Requirements
For the Bachelor of Computer Science and Engineering
June 21, 2026

Name of the student: Milán Székely
Final project course: CSE3000 Research Project
Thesis committee: Arash Asadi, Florian Kosterhon, George Iosifidis

***Abstract*—Reliable positioning is essential for autonomous drones, yet global navigation satellite systems (GNSS) can become unreliable or unavailable. This work compares passive RF-based methods for estimating distance and relative radial velocity with a single unsynchronized receiver. Calibrated RSSI ranging and direct Doppler estimation are selected as lightweight approaches and evaluated using an RFSoC 4x2-based prototype with a continuous-wave signal. Under controlled indoor conditions, calibrated RSSI achieves a mean absolute percentage error of 6.3% over the tested positions, although antenna orientation changes RSSI by almost $7\ \mathrm{dB}$ at a fixed distance. Doppler estimation, with clock offset estimated from stationary measurements before and after motion, recovers the correct motion direction in all motion trials and achieves a mean absolute error of $0.33\ \mathrm{m/s}$. The motion-trial RMSE and the stationary null-test standard deviation were both $0.43\ \mathrm{m/s}$, suggesting that imperfect clock-offset compensation and estimator uncertainty account for a substantial part of the radial-velocity estimation error. The results show that both methods provide lightweight distance and radial-velocity features, but their accuracy is limited by propagation conditions and oscillator stability.**

I. Introduction

RELIABLE positioning is essential for autonomous drone operation. Most unmanned aerial vehicles (UAVs) rely heavily on global navigation satellite systems (GNSS) for absolute localization, but GNSS can become unreliable or unavailable in obstructed environments or under jamming and spoofing attacks [1], [2]. In such GNSS-denied scenarios, common alternative navigation approaches include inertial navigation, vision-based localization, LiDAR-based mapping, radar, and dedicated radio-frequency (RF) ranging [1], [2]. However, these alternatives also have limitations: inertial navigation accumulates error over time, vision- and LiDAR-based methods depend strongly on environmental conditions, such as lighting, weather, and visibility, while radar and dedicated RF ranging require transmission and may therefore increase detectability [1], [3].

A complementary approach is to exploit signals of opportunity: ambient radio signals, such as cellular, Wi-Fi, or broadcast transmissions, that are already present in the environment. Because the receiver only observes existing signals and does not transmit, this approach is attractive for applications in which low detectability is important. Prior work has shown that signals of opportunity can support navigation in GNSS-denied environments and complement inertial systems by providing external measurements [2].

This work focuses on estimating distance and relative radial velocity between a single transmitter and a passive, unsynchronized receiver. Existing estimation methods impose different requirements: time-based methods require timing information and synchronized infrastructure [4], [5], phase-based methods require phase ambiguity resolution or continuous phase observations [6], [7], and model-based RSSI ranging requires environment-specific propagation calibration [8], [9]. Doppler-based methods avoid timing synchronization, but require transmitter–receiver clock effects to be estimated and compensated [2], [10]. These differences motivate a comparison under the constraints of a single passive receiver, with emphasis on methods that require limited signal knowledge and low computational complexity.

The research is guided by the following sub-questions:

- What passive RF-based methods exist for estimating distance and relative radial velocity, and what requirements do they impose?
- Which methods are suitable for a passive receiver with limited computational complexity and signal knowledge?
- How accurate and stable are the selected methods under controlled laboratory conditions, considering effects such as multipath, antenna orientation, clock offset, and clock drift?

The main contribution of this work is a comparison of passive RF-based distance and relative radial velocity estimation methods, followed by the implementation and evaluation of two lightweight approaches on an RFSoC 4x2-based prototype. Calibrated RSSI ranging is examined for coarse distance estimation, while direct frequency-offset estimation is evaluated for Doppler-based relative radial velocity estimation. The prototype is tested under controlled laboratory conditions using a continuous-wave signal. The resulting accuracy, stability, and practical limitations are assessed experimentally.

The remainder of this paper is structured as follows. Section II introduces the system model and the relevant RF background. Section III compares passive RF-based distance and velocity estimation methods. Section IV describes the RFSoC 4x2-based prototype receiver pipeline. Section V presents the experimental evaluation. Section VI discusses the results, limitations, and future work. Section VII reflects on responsible research, and Section VIII concludes the paper.

II. Background and System Model

This section defines the passive transmitter–receiver setup and introduces the signal quantities used by the distance and velocity estimators.

A. System Model

The considered system consists of a single transmitter and a passive receiver. In the target scenario, the transmitter is an existing communication source, such as a Wi-Fi access point, a cellular base station, or a broadcast transmitter. The receiver does not control this transmitter or transmit a probing signal itself; it only observes the received RF signal and therefore remains fully passive. The receiver is assumed to know basic signal parameters needed for tuning and processing, such as the carrier frequency or approximate bandwidth, but not necessarily the transmitted data symbols.

B. Propagation Delay

Time-based ranging methods rely on the one-way propagation delay $\tau(t) = d(t)/c$, where $d(t)$ is the transmitter–receiver distance and c is the speed of light.

C. Received Power and Path Loss

RSSI-based ranging uses received signal power as an indirect distance cue [8]. A common large-scale propagation model is the log-distance path-loss model [11, p. 102],

$$P_r(d) = P_r(d_0) - 10n \log_{10}\left(\frac{d}{d_0}\right), \tag{1}$$

where $P_r(d)$ is the received power in decibels at distance d, d_0 is a reference distance, and n is the path-loss exponent. The exponent depends on the environment: in free space, $n \approx 2$, whereas indoor measurements can deviate significantly due to reflections, antenna orientation, and multipath [9].

D. Doppler and Clock Effects

Relative radial motion shifts the received carrier frequency due to the Doppler effect. With the sign convention $v_r(t) > 0$ corresponding to motion away from the transmitter, the Doppler shift for a carrier frequency f_c is approximately [11, p. 141]

$$f_D = -\frac{v_r}{c} f_c = -\frac{v_r}{\lambda}, \tag{2}$$

where c is the speed of light and $\lambda = c/f_c$ is the carrier wavelength.

In practice, the measured frequency offset after downconversion is not solely due to Doppler. Independent transmitter and receiver oscillators introduce clock offset, so the measured frequency offset is modeled as [10]

$$\hat{f}_{\text{off}} \approx f_D + f_{\text{clk}}, \tag{3}$$

where f_{clk} represents the clock offset between the transmitter and receiver oscillators. Clock drift causes this offset to change over time, so a static calibration is only valid for a limited interval [2], [10]. Any change in f_{clk} appears as an additional frequency shift and can therefore be confused with Doppler, making clock stability a central limitation for Doppler-based velocity estimation.

III. Related Work

Passive RF-based localization and motion estimation can use several types of signal measurements, including received signal strength, propagation delay, carrier phase, and Doppler shift. These measurements differ in the information they provide, the requirements they impose, and the complexity of the receiver processing. This section reviews the main method families relevant to estimating distance and relative radial velocity from passive signals of opportunity, with emphasis on their suitability for a lightweight receiver using a single transmitter and no transmitter–receiver synchronization.

A high-level overview is given in Table I. The remainder of the section discusses each method family in turn and concludes by identifying the approaches used in the prototype.

A. Distance Estimation Methods

1) RSSI-based methods: RSSI-based ranging uses received signal power as a distance-related feature. Several variants exist. Model-based methods fit a propagation model and then invert it to estimate distance. A common example is the log-distance path-loss model [11, p. 102], introduced in (1). Fingerprinting methods instead compare measured RSSI values against a pre-recorded map of the environment, as in the RADAR indoor localization system [12]. RSSI can also be used more qualitatively: because received power generally decreases with distance, changes in RSSI can indicate whether the receiver is moving closer to or farther from the transmitter, without requiring accurate absolute ranging.

Model-based RSSI ranging is attractive because it requires little signal knowledge and can be implemented solely from received-power measurements. Patwari et al. [8] treat received signal strength as one of the basic measurement types for wireless localization and discuss how it can be related to distance through a path-loss model. Seidel and Rappaport [9] show through indoor measurements that path-loss behavior depends strongly on the building environment, which motivates calibration of the path-loss exponent. Zhou and Pollard [13] use RSSI for Bluetooth-based positioning and show that it can provide coarse position information, although the measurements are sensitive to local signal fluctuations.

Fingerprinting-based RSSI methods use the same received-power measurements differently. Instead of directly fitting a propagation model, they compare measured RSSI values against a previously collected radio map [12]. This can improve position estimation in a known environment, but it requires environment-specific training data and therefore does not transfer easily to a new location.

More generally, survey papers emphasize both the simplicity and the limitations of RSSI-based localization. Boukerche et al. [4] and Liu et al. [5] discuss RSSI as a low-cost measurement type, but also note its sensitivity to the propagation environment. Multipath, antenna orientation, transmit-power variation, and receiver-gain changes can all produce power changes unrelated to distance.

For this work, fingerprinting is not suitable because it requires a prior radio map of the environment, which conflicts with the goal of a portable prototype. A calibrated path-loss model is more appropriate because it requires only a small number of reference measurements and can be implemented with a simple received-power estimate. RSSI is therefore selected as a lightweight baseline for coarse distance estimation, but not as a high-accuracy ranging method.

2) Time-based methods: Time-based ranging estimates the distance from the propagation delay. Time of arrival (ToA) uses the absolute delay between transmission and reception, while time difference of arrival (TDoA) uses differences between arrival times. Since propagation delay is directly related to distance, time-based methods can provide higher ranging accuracy than RSSI when sufficient bandwidth and synchronization are available [4], [5].

TABLE I
HIGH-LEVEL COMPARISON OF PASSIVE RF-BASED DISTANCE AND RELATIVE RADIAL VELOCITY ESTIMATION METHODS

Method	Quantity	Main assumptions	Main limitations	Complexity
RSSI-based ranging	Distance	Stable transmit power, fixed receiver gain, calibrated propagation model	Sensitive to multipath, antenna orientation, and environment-specific calibration	Low
ToA	Distance	Known transmission time and tight TX–RX synchronization, sufficient bandwidth	Difficult with an unsynchronized, uncooperative transmitter	Medium
TDoA	Position	Multiple synchronized receivers or transmitters with known timing relations	Requires additional synchronized infrastructure	Medium
Phase-based ranging	Distance	Phase measurements across multiple carrier frequencies or continuous phase tracking	Ambiguous modulo wavelength, sensitive to multipath	High
Direct Doppler	Velocity	Stable or calibratable clock offset	Clock offset and clock drift are indistinguishable from Doppler without calibration	Low
Carrier phase tracking	Velocity	Continuous phase tracking, cycle-slip handling, stable clocks	Requires uninterrupted phase continuity, phase errors are accumulated	High

The main challenge is the required timing reference. One-way ToA requires knowledge of the transmit time and tight synchronization between transmitter and receiver. TDoA reduces the need for direct transmitter–receiver synchronization, but requires multiple synchronized receivers or multiple transmitters with known timing relations. Chan and Ho [14] show how TDoA measurements can be used for hyperbolic localization once such infrastructure is available. In the single-transmitter, single passive receiver setup considered in this work, however, these timing or infrastructure requirements are not available. Time-based methods are therefore less aligned with the chosen system model, although they remain highly relevant when the synchronized infrastructure is available.

3) Phase-based ranging: Phase-based ranging uses the carrier phase to infer distance or displacement. As a signal propagates over a distance d, its carrier phase changes by approximately $2\pi d/\lambda$, where λ is the carrier wavelength. Therefore, changes in measured phase can be converted to changes in propagation distance, and, if the phase ambiguity is resolved, to absolute range. Because phase can be measured very precisely, phase-based systems can achieve much finer resolution than RSSI under favorable conditions. Zand et al. [6] and Schröder and Wolf [7] demonstrate that phase information can support accurate short-range ranging when phase ambiguity and measurement conditions are controlled.

The main limitation is that the single-frequency carrier phase is ambiguous modulo 2π, corresponding to an ambiguity of one wavelength in distance. Practical systems therefore need additional information to resolve this ambiguity, such as phase measurements across multiple carrier frequencies [6], [7] or continuous phase tracking from a known state. These assumptions are difficult to satisfy in the single-transmitter passive setup considered here, where the receiver does not control the transmitted frequency and cannot guarantee uninterrupted phase observations. Phase is also sensitive to multipath and oscillator phase offsets. Therefore, phase-based ranging is not compatible with the chosen system model unless additional assumptions are introduced.

B. Velocity Estimation Methods

1) Direct Doppler estimation: Direct Doppler estimation uses the frequency shift caused by relative radial motion, following the relation in (2). This makes it well-suited for passive sensing, as the receiver does not need to estimate absolute propagation delay or decode the full signal; it only needs a stable spectral component whose frequency can be tracked. Signals-of-opportunity navigation work shows that Doppler measurements can provide useful navigation information, but also that they must be separated from transmitter and receiver clock effects [2], [10].

Different signal types require different practical frequency estimators. For a continuous-wave or narrowband single-tone signal, an FFT peak estimate with interpolation or a single-tone estimator, such as Kay's estimator [15], can be used. For OFDM signals, Moose [16] and Schmidl–Cox [17] estimate carrier-frequency offset from repeated or cyclic OFDM structure. In all cases, the estimated frequency offset is used as the measurement from which radial velocity is obtained after clock compensation.

The required frequency precision is demanding because Doppler shifts are small at communication carrier frequencies. For example, at $f_c = 2.4$ GHz, a radial velocity of $1\ \mathrm{m/s}$ corresponds to a Doppler shift of about 8 Hz. In practice, the dominant limitation is often the stability of the transmitter and receiver frequency references. As modeled in (3), clock offset and drift are indistinguishable from Doppler unless they are calibrated, modeled, or otherwise compensated. This makes direct Doppler attractive for a lightweight receiver, but makes clock compensation essential.

2) Carrier phase tracking: Carrier phase tracking uses the accumulated phase of a received carrier to estimate motion. Since frequency is the time derivative of phase, a continuously tracked carrier phase can be used to estimate carrier frequency shift and therefore relative radial velocity. This principle is used by Ding and Wang [18] for velocity estimation with GPS receivers.

The main requirement is continuous and reliable phase tracking. Practical systems must handle phase ambiguity, cycle

slips, oscillator phase noise, and clock errors. These requirements are difficult to satisfy for an unsynchronized passive receiver, especially when phase continuity cannot be guaranteed. Carrier phase tracking is therefore most appropriate when the receiver can maintain a continuous phase lock and when phase ambiguities can be resolved.

C. Summary of Method Suitability

The reviewed methods differ mainly in their requirements. Under the system model considered in this work, the most suitable methods are those that can operate with a single passive receiver, require limited knowledge of the transmitted signal, and can be implemented with lightweight operations on the captured samples.

For distance estimation, calibrated RSSI ranging is the most suitable method under these constraints. It only requires received-power estimation and a small calibration procedure, whereas the other reviewed methods require timing synchronization, additional synchronized infrastructure, transmitter-controlled frequency changes, or continuous phase tracking. Its main limitation is that it provides only coarse distance information and depends strongly on the propagation environment.

For relative radial velocity estimation, direct Doppler estimation is the most suitable method under these constraints. It directly relates frequency offset to radial velocity and can be implemented using standard frequency-estimation techniques. Its main limitation is that the Doppler shift must be separated from transmitter–receiver clock offset and drift.

The remaining method families are relevant when transmitter–receiver synchronization, multiple synchronized receivers, or continuous phase tracking are available, but these conditions are not available in the system model used here.

IV. Implementation

This section describes the prototype receiver pipeline implemented on the RFSoC 4x2 platform. The implementation consists of three main parts: the RFSoC capture architecture, the signal processing pipeline, and the estimators for distance and relative radial velocity. It provides the experimental platform for evaluating calibrated RSSI ranging and direct Doppler estimation under controlled laboratory conditions.

A. Platform and Capture Architecture

The receiver is implemented on an AMD RFSoC 4x2 development board, which integrates RF data converters, programmable logic (PL), and a processing system (PS) running PYNQ. The capture architecture is based on the existing RFSoC-MTS project [19]. This work extends that design for the present receiver pipeline by adding digital downconversion to complex baseband and by capturing I/Q samples instead of real-valued samples.

Captured I/Q samples are transferred over an AXI-Stream data path and written to memory. Two capture paths are used. A short-capture path stores samples in the on-chip block RAM (BRAM), providing short windows for rapid inspection and RSSI estimation. A deep-capture path writes samples to the board's PL-attached DDR4 memory (DRAM) using direct memory access (DMA). The deep-capture path enables capturing several milliseconds, which are needed for accurate frequency estimation in the Doppler experiments.

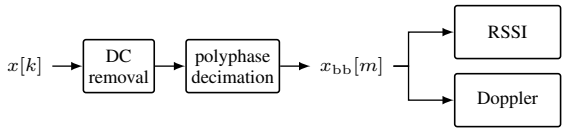

Fig. 1. Software preprocessing pipeline. The captured complex samples $x[k]$ are DC-corrected and polyphase-resampled to produce the decimated baseband signal $x_{\mathrm{bb}}[m]$, which is used by both estimators.

B. Signal Processing Pipeline

All signal processing is performed in software on the PS using Python. Raw I/Q samples are read from memory and assembled into the complex baseband sequence $x[k] = I[k] + jQ[k]$. The same preprocessing pipeline, shown in Fig. 1, is then applied before both RSSI and Doppler estimation.

First, the sample mean is subtracted to remove DC offset caused by local-oscillator leakage and converter bias. The signal is then resampled using a polyphase finite impulse response (FIR) filter, which combines anti-alias low-pass filtering and decimation in a single operation. Decimation reduces the number of samples processed by downstream estimators, while the achievable frequency resolution is still primarily determined by the observation duration rather than the post-decimation sample rate. The polyphase implementation is efficient because it computes only the output samples retained after decimation, rather than filtering the full-rate signal and then discarding samples.

C. RSSI and Distance Estimation

RSSI is computed from the preprocessed complex baseband samples $x_{\mathrm{bb}}[m]$. Since received power is proportional to the squared magnitude of the complex signal [11, pp. 148–149], the average received-power estimate over a window of M samples is

$$\hat{p}_r = \frac{1}{M} \sum_{m=0}^{M-1} |x_{\mathrm{bb}}[m]|^2 . \tag{4}$$

The corresponding RSSI estimate in decibels relative to full scale (dBFS) is

$$\hat{P}_r = 10 \log_{10} \left(\frac{\hat{p}_r}{p_{\mathrm{FS}}} \right), \tag{5}$$

where p_{FS} is the ADC full-scale reference power. The dBFS value is a relative digital power measure rather than an absolute received-power measurement in dBm. This is sufficient for the calibrated path-loss model because only relative changes in received power are used.

Distance estimation requires calibration of the path-loss model for the measurement environment. RSSI is measured at known reference distances d_i, giving calibration pairs $(d_i, \hat{P}_r(d_i))$, where $\hat{P}_r(d_i)$ is the measured RSSI in dBFS. The calibration measurements are fitted to the log-distance

model in (1) using least-squares regression, giving estimates $\hat{P}_r(d_0)$ of the reference RSSI and $\hat{n}$ of the path-loss exponent. After calibration, a new RSSI measurement $\hat{P}_r$ is mapped to distance by inverting the fitted model:

$$\hat{d} = d_0 \cdot 10^{\left(\hat{P}_r(d_0) - \hat{P}_r\right)/(10\hat{n})}. \tag{6}$$

D. Frequency and Velocity Estimation

Radial velocity is estimated from the residual frequency offset of the baseband tone using the Doppler relation in (2). Two frequency estimators are implemented. The first is an FFT-based estimator that locates the spectral peak and refines it using parabolic interpolation. The second is Kay's estimator [15], which estimates the frequency of a single complex tone from the phase progression of the samples. Kay's estimator is used as the primary estimator in the single-tone experiments because it matches the signal model in this paper and can provide more accurate frequency estimates than a simple FFT peak estimate for the same observation window. The FFT-based estimator is only used as a consistency check.

As discussed in Section III-B, Doppler shifts at walking speeds are small. At $f_c = 2.41$ GHz, $1\ \mathrm{m/s}$ of radial velocity corresponds to approximately 8 Hz. Estimating such small frequency shifts requires sufficiently long observation windows, because longer captures provide more samples and generally reduce the variance of single-tone frequency estimates [15]. This motivates the use of the deep-capture DRAM path for Doppler measurements. The capture duration is selected experimentally in Section V-B as a compromise between frequency-estimation stability and processing cost.

Because the transmitter and receiver use independent oscillators, the measured baseband frequency includes the clock term f_{clk} in (3). To reduce this effect, each velocity measurement uses three consecutive measurement groups: a static reference before motion, a motion interval, and a static reference after motion. Each group can contain multiple captures. For each group, the estimated frequencies and capture timestamps are averaged to obtain one representative frequency and time. Let these averaged values be $(\bar{f}_b, \bar{t}_b)$, $(\bar{f}_m, \bar{t}_m)$, and $(\bar{f}_a, \bar{t}_a)$, respectively. The frequency during the motion interval is estimated by linear interpolation between the two static reference groups:

$$\hat{f}_{\mathrm{clk}}(\bar{t}_m) = \bar{f}_b + \frac{\bar{f}_a - \bar{f}_b}{\bar{t}_a - \bar{t}_b}(\bar{t}_m - \bar{t}_b). \tag{7}$$

The Doppler component is then estimated as

$$\hat{f}_D = \bar{f}_m - \hat{f}_{\mathrm{clk}}(\bar{t}_m), \tag{8}$$

and converted to radial velocity using (2).

This bracketing approach assumes that the clock drift is approximately linear over the short interval between the two static reference groups. This assumption is evaluated experimentally in Section V-B. The method also requires the reference groups to contain no motion-induced Doppler shift; in the experiments, this is enforced by acquiring the reference captures while the receiver is stationary.

E. Lightweight Implementation Considerations

The selected estimators are lightweight in terms of arithmetic complexity. RSSI estimation requires only squaring, accumulation, and averaging of complex samples. Doppler estimation in the single-tone setup requires estimating the frequency of a single narrowband component, followed by interpolation for clock-offset compensation and conversion from frequency shift to radial velocity. These operations are simpler than methods requiring precise timing synchronization, phase ambiguity resolution, or continuous phase tracking.

F. Implementation Artifacts

The implementation artifacts developed for this work are publicly available in an accompanying GitHub repository [20]. The repository contains the sources required to reconstruct the Vivado block design, the Python signal-processing and estimation code, and the Jupyter notebooks used for the experiments and evaluation. It also includes matching bitstream, hardware-description, and device-tree files for deployment on the RFSoC 4x2.

V. Evaluation

This section evaluates the prototype under controlled laboratory conditions and addresses the third research sub-question: how accurate and stable the selected methods are in the presence of practical effects, such as multipath, clock offset, and clock drift. Three main experiments are reported: RSSI-based distance estimation, clock-drift characterization, and Doppler-based velocity estimation.

All experiments used the receiver pipeline described in Section IV. A USRP software-defined radio (SDR) transmitted a continuous-wave tone near $f_c = 2.41$ GHz, offset by approximately 100 kHz, while the RFSoC 4x2 received the signal with an ADC sampling rate of $4\ \mathrm{GS/s}$, downconverted by 2.41 GHz. The transmitter and receiver used independent oscillators and were not synchronized. Measurements were performed indoors in a laboratory room with line-of-sight between transmitter and receiver. The room layout and RSSI measurement positions are shown in Fig. 2. Photographs of the transmitter and receiver setups are provided in Appendix A. This environment is useful for controlled testing, but challenging for RSSI-based ranging because reflections from walls, desks, shelves, and equipment can cause strong multipath.

A. RSSI-Based Distance Estimation

The RSSI experiment evaluates whether a calibrated log-distance path-loss model can provide coarse distance estimates in the laboratory environment. The USRP transmitter was placed at a fixed position, and the receiver was placed at known calibration and test locations. The RSSI value at each location was computed from 100 captures; the reported standard deviation is the variation across these captures.

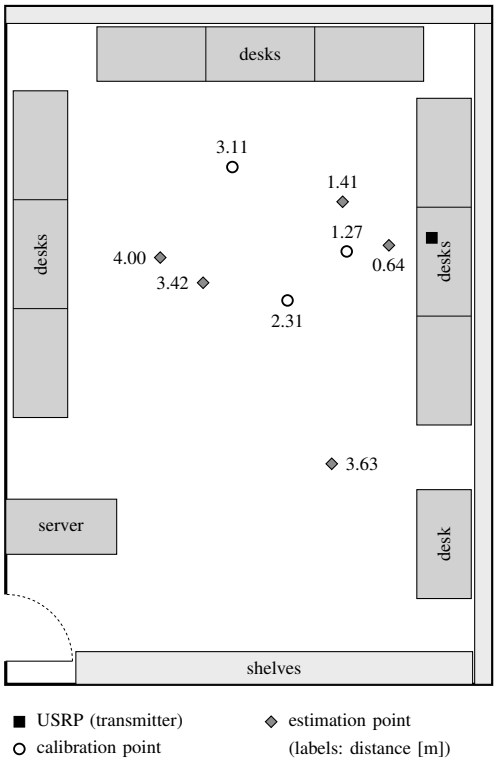

Fig. 2. Laboratory layout used for the experiments. The transmitter position, RSSI calibration points, and RSSI estimation points are marked. Labels indicate the true transmitter–receiver distance in meters.

TABLE II
RSSI CALIBRATION MEASUREMENTS

Distance [m]	RSSI [dBFS]	Std [dB]
1.27	−19.929	0.097
2.31	−23.633	0.211
3.11	−26.455	0.171

1) Path-loss model: The path-loss model was calibrated using three reference measurements. Table II summarizes the calibration data. Fitting the log-distance model by least-squares regression gives a reference RSSI of $\hat{P}_r(1\ \mathrm{m}) = -18.09\ \mathrm{dBFS}$ and a path-loss exponent of $\hat{n} = 1.64$. Although $\hat{n} = 1.64$ is below the free-space value of 2, it lies within the typical range of 1.6 to 1.8 reported for indoor line-of-sight environments [11, p. 104]. The fitted model is shown in Fig. 3.

The calibrated model was then inverted to estimate distance from RSSI at five test locations. The results are shown in Table III. The mean absolute error over the five test points is 0.18 m, corresponding to a mean absolute percentage error of 6.3%. The largest error occurs at the 3.42 m test point, where the distance is overestimated by 12.0%. Overall, the results show that calibrated RSSI can provide useful coarse distance estimates in the tested setup, but the accuracy remains dependent on the local propagation conditions.

2) Antenna-orientation sensitivity: A separate fixed-distance test was performed to check the effect of receiver antenna orientation. The receiver was kept at a distance of 1 m from the transmitter, while the receiver orientation was changed. The measured RSSI varied from approximately −16.49 dBFS to −23.38 dBFS, a range of almost 7 dB. With the fitted path-loss exponent $\hat{n} = 1.64$, such a change corresponds to a distance factor of approximately $10^{7/(10\hat{n})} \approx 2.7$ in the calibrated path-loss model. Therefore, antenna orientation alone could change the inferred distance by a factor of approximately 2.7, even though the true distance is unchanged. This confirms that antenna orientation is a major source of RSSI variation and can produce power changes unrelated to distance. RSSI-based ranging should therefore be interpreted as a coarse, calibration-dependent distance feature rather than as a precise ranging method.

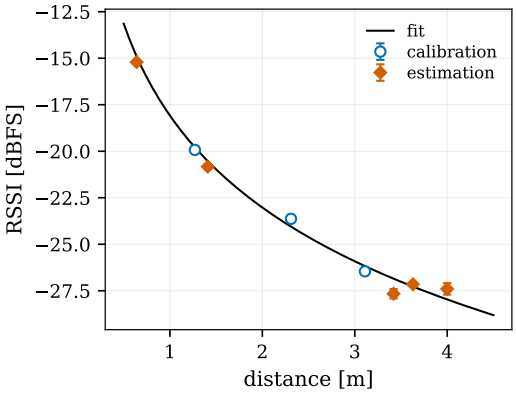

Fig. 3. Calibrated RSSI path-loss model fitted from three reference measurements.

TABLE III
RSSI-BASED DISTANCE ESTIMATION RESULTS

True [m]	RSSI [dBFS]	Est. [m]	Error
0.64	-15.21 ± 0.05	0.668 ± 0.005	+4.4%
1.41	-20.83 ± 0.11	1.470 ± 0.022	+4.3%
3.42	-27.66 ± 0.26	3.831 ± 0.136	+12.0%
3.63	-27.15 ± 0.08	3.568 ± 0.039	−1.7%
4.00	-27.40 ± 0.31	3.644 ± 0.159	−8.9%

B. Clock-Drift Characterization

Doppler-based velocity estimation is affected by the frequency stability of the independent transmitter and receiver oscillators. When both devices are stationary, the true Doppler shift is zero, so any changes in the measured baseband tone frequency are due to estimator uncertainty and clock drift. Two stationary experiments were therefore performed. The first evaluates how the frequency estimate depends on capture duration. The second uses the selected capture duration to characterize clock drift over time.

1) Capture duration: The first experiment examines the effect of capture length on frequency-estimation stability in order to select an operating point. For each capture length, 60 consecutive captures were acquired over 3 s while both devices remained stationary, and the tone frequency was estimated

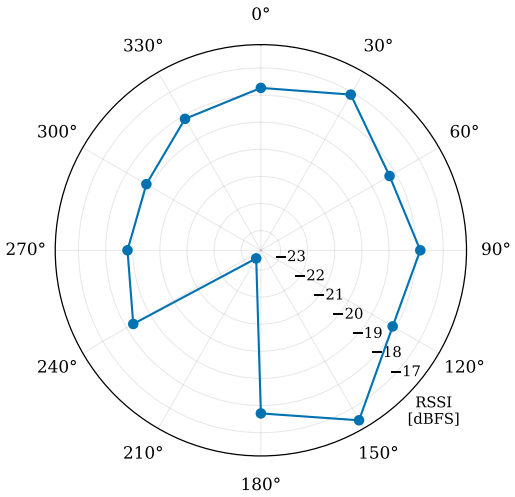

Fig. 4. Effect of receiver antenna orientation on RSSI at a fixed transmitter–receiver distance of 1 m.

TABLE IV
FREQUENCY STABILITY VERSUS CAPTURE LENGTH

Samples	Capture [ms]	Residual [Hz]
8×2^{20}	2.10	69.4
9×2^{20}	2.36	63.7
16×2^{20}	4.19	12.8
30×2^{20}	7.86	9.8

from each capture. Because the true Doppler shift is zero, variation in the estimates is caused by frequency-estimation uncertainty and clock drift. A linear drift trend was fitted and removed, after which the residual standard deviation was used as a measure of short-term frequency stability. The results are summarized in Table IV.

Increasing the capture duration from 2.36 ms to 4.19 ms reduces the residual standard deviation from approximately 64 Hz to 13 Hz, showing that the shortest captures are strongly affected by frequency-estimation uncertainty. Increasing the duration further to 7.86 ms reduces the residual only slightly, to approximately 10 Hz, suggesting that oscillator instability becomes the dominant limitation beyond 4 ms. Longer captures also increase data volume, processing cost, and proximity to the platform's per-buffer DMA transfer limit. A capture length of 16×2^{20} samples, corresponding to approximately 4.2 ms, is therefore used for the remaining experiments as a practical compromise between frequency stability and processing cost.

2) Clock drift over time: After selecting the capture duration, the tone frequency was measured repeatedly over short and longer stationary intervals. These measurements test the assumption behind the bracketing procedure in Section IV-D: over the short interval between the two static reference groups, the clock offset should be approximated reasonably by linear interpolation. The measured traces are shown in Fig. 5.

The short-window measurements show that, over the 2.5 s

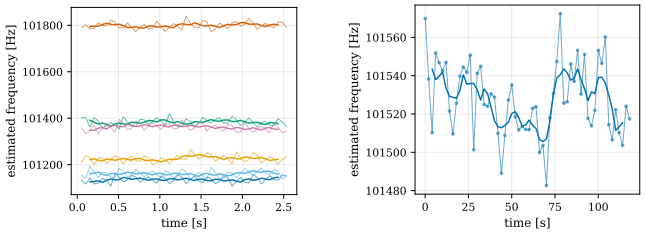

(a) Short-timescale measurement: six 2.5 s trials.

(b) Long-timescale measurement: one 2 min trial.

Fig. 5. Clock-drift characterization with the transmitter and receiver stationary. The bold curves show a 5-sample moving average.

interval used in each trial, the estimated frequency remains approximately constant, with only small short-term fluctuations. The absolute frequency offset differs across trials, confirming that a single static calibration would not be reliable over longer periods. However, the short-term stability supports the use of before–after bracketing, as the clock offset during the motion capture can be approximated from two nearby static reference groups.

This does not remove clock drift as a limitation. If the drift becomes nonlinear within the bracketing interval, or if short-term fluctuations occur during the motion capture, the interpolated reference will be imperfect, and the remaining frequency error will be interpreted as Doppler.

C. Doppler-Based Velocity Estimation

Velocity was estimated using the clock-offset bracketing procedure from Section IV-D. In all Doppler experiments, each of the before, motion, and after measurement groups consisted of four consecutive captures. The frequency estimates and timestamps from these four captures were averaged to obtain the representative frequency and time for each group. Two tests are reported: a stationary null test, in which the true radial velocity is zero, and motion trials, in which the receiver was moved toward or away from the transmitter.

1) Null test: A stationary null test was first performed to evaluate the full Doppler pipeline under the condition that the true radial velocity is zero. In this test, the receiver was kept stationary, but the same before–after bracketing procedure was applied as in the motion experiments. Therefore, any nonzero velocity estimate is caused by imperfect clock-offset compensation, estimator uncertainty, or small environmental changes during the measurement. Across 10 trials, the estimated velocity had a mean of $+0.01$ m/s and a standard deviation of 0.43 m/s. The individual estimates are listed in Appendix B and are also shown together with the motion-trial results in Fig. 6. These results indicate that the bracketing procedure does not introduce a significant bias in the stationary case and provide a baseline uncertainty for interpreting the motion trials.

2) Motion trials: The receiver was then mounted on a cart and moved manually in a straight line toward or away from the transmitter. Reference velocities were estimated from

TABLE V
DOPPLER-BASED RADIAL VELOCITY ESTIMATION RESULTS

Trial	v_{ref} [m/s]	$\hat{v}$ [m/s]	Error [m/s]
1	−0.74	−0.449	+0.291
2	+0.87	+1.812	+0.942
3	−0.67	−0.803	−0.133
4	+0.83	+0.659	−0.171
5	−0.95	−0.615	+0.335
6	+0.87	+0.914	+0.044
7	−1.67	−2.049	−0.379
8	+1.67	+2.470	+0.800
9	−0.87	−1.110	−0.240
10	+1.11	+1.402	+0.292
11	−1.33	−1.004	+0.326
12	+1.43	+1.489	+0.059

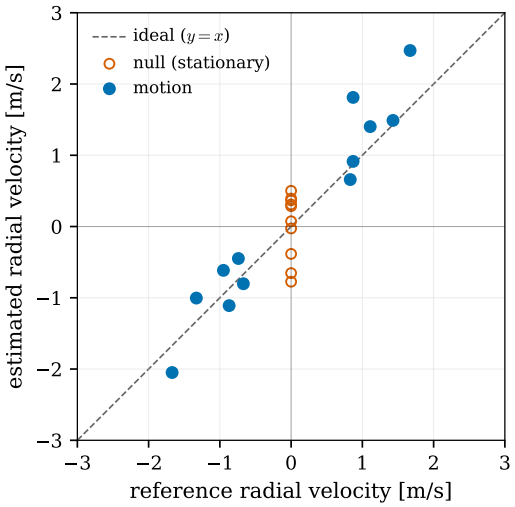

Fig. 6. Estimated radial velocity for the stationary null test and motion trials. Motion-trial reference velocities were obtained from video timing, while the null-test reference velocity is zero.

phone video recordings over a known distance, assuming approximately constant speed during each trial. These values provide approximate rather than high-precision ground truth.

Table V shows the radial velocity estimates. Across all twelve motion trials, the sign of the estimated velocity matches the sign of the reference velocity, meaning that motion toward and away from the transmitter was consistently distinguished. The mean absolute error is $0.33\ \mathrm{m/s}$, and the root mean square error is $0.43\ \mathrm{m/s}$. The largest errors occur in trials 2 and 8, where the velocity is overestimated by $0.94\ \mathrm{m/s}$ and $0.80\ \mathrm{m/s}$, respectively. These errors are consistent with the sensitivity of Doppler estimation to imperfect clock-offset compensation and with the limited accuracy of the video-based reference.

VI. DISCUSSION AND FUTURE WORK

The RSSI results show that calibrated received power can provide coarse distance information under controlled conditions. However, the almost $7\ \mathrm{dB}$ variation caused by antenna orientation at a fixed distance demonstrates that RSSI is not inherently robust. Rotating the receiver and selecting the strongest received-power direction may improve repeatability, although multipath would remain a limitation [5], [8]. Orientation-aware measurements, controlled antenna placement, and outdoor line-of-sight experiments should therefore be investigated.

For Doppler estimation, oscillator stability and estimator uncertainty are the main practical limitations. Longer captures improved frequency stability only up to a point, while the short-term drift measurements supported local before–after bracketing. However, this approach still assumes that the clock offset varies smoothly over the bracketing interval and cannot fully compensate for nonlinear drift or short-term fluctuations. Future work should therefore investigate dynamic clock-offset tracking, for example, using a Kalman filter [10].

The motion trials recovered the correct direction of motion, but the video-based reference velocities were approximate. The motion-trial RMSE and stationary null-test standard deviation were both $0.43\ \mathrm{m/s}$, suggesting that imperfect clock-offset compensation and estimator uncertainty account for a substantial part of the observed error. Future experiments should use a motorized track or a motion-capture system to measure velocity more accurately and control it across repeated trials.

Finally, the prototype was tested with a controlled continuous-wave tone, and all estimation was performed in software on the processing system. Future work should extend the prototype to modulated OFDM signals, such as Wi-Fi, 4G, 5G, or DVB-T, and move the lightweight estimators to the FPGA fabric for continuous real-time operation.

VII. RESPONSIBLE RESEARCH

This work follows the principles of the Netherlands Code of Conduct for Research Integrity, with emphasis on transparency, reproducibility, and responsible use. Transparency is supported by clearly separating the existing RFSoC-MTS base design from the extensions made in this work, and by citing the original repository. To support reproducibility, the hardware design sources, signal-processing code, and experiment notebooks developed for this work are publicly available in an accompanying GitHub repository [20]. Reproducibility is further supported by the use of commercially available hardware, open-source software, and documented calibration and evaluation procedures. Because RF measurements depend on setup-specific effects such as antenna placement, multipath, receiver gain, and clock drift, the exact RSSI values and frequency offsets are not expected to reproduce identically across sessions. Instead, reproducible outcomes include the calibration procedures and the relative accuracy and precision trends.

The work also has dual-use implications. Passive navigation in GNSS-denied environments can support civilian applications, but the same low-detectability sensing methods could also be used for surveillance or military purposes. This work does not introduce new sensing principles, but it may lower implementation barriers by comparing and prototyping

lightweight methods. The experiments were limited to controlled measurements in the unlicensed 2.4 GHz band; no real communication content was intercepted, no personal data was collected, and only signal power and frequency were used.

AI tools were used only for language-level support, such as rephrasing and improving readability. They were not used to generate the ideas, methods, experimental design, or results. All technical content, results, and conclusions were checked and remain the responsibility of the author.

VIII. Conclusion

This work compared passive RF-based methods for distance and relative radial velocity estimation under the constraints of a single passive, unsynchronized receiver. The related-work analysis compared RSSI-based, time-based, phase-based, and Doppler-based approaches. Calibrated RSSI ranging and direct Doppler estimation were selected as the methods most compatible with the considered system model and implemented in an RFSoC 4x2-based prototype.

The experiments show that both selected methods are feasible under controlled laboratory conditions. Calibrated RSSI provided coarse distance estimates with a mean absolute percentage error of 6.3% over the tested positions. However, the antenna-orientation experiment showed that rotation alone can change RSSI by almost 7 dB at a fixed distance. RSSI is therefore useful as a coarse, calibration-dependent distance feature, but not as a precise ranging method in reflective or changing environments.

Direct Doppler estimation with clock-offset bracketing recovered the correct direction of radial motion in all 12 motion trials. The estimates achieved a mean absolute error of 0.33 m/s and a root mean square error of 0.43 m/s against approximate video-based reference velocities. The stationary null test produced a standard deviation of 0.43 m/s, providing an empirical measure of the combined effects of imperfect clock-offset compensation, estimator uncertainty, and other unmodelled measurement effects.

Overall, calibrated RSSI and direct Doppler can provide lightweight distance and radial-velocity features for a passive receiver, but their practical accuracy depends strongly on propagation conditions and oscillator stability.

Appendix A
Experimental Setup Photographs

The laboratory equipment used in the experiments is shown in Fig. 7.

(a) RFSoC receiver setup on the cart. (b) Fixed USRP transmitter setup.

Fig. 7. Laboratory equipment used for the experiments.

Appendix B
Doppler Null-Test Trials

Table VI lists the individual stationary null-test trials, in which the receiver was held stationary so that the true radial velocity is zero. Across the 10 trials, the estimated radial velocity has a mean of $+0.01$ m/s and a standard deviation of 0.43 m/s, showing no significant observed bias under the tested conditions.

TABLE VI
Stationary Null-Test Trials

Trial	$\hat{v}$ [m/s]
1	-0.774
2	$+0.074$
3	$+0.367$
4	-0.027
5	-0.384
6	$+0.286$
7	-0.654
8	$+0.392$
9	$+0.310$
10	$+0.501$

References

[1] S. Alghamdi, S. Alahmari, S. Yonbawi, K. Alsaleem, F. Ateeq, and F. Almushir, "Autonomous navigation systems in GPS-denied environments: A review of techniques and applications," in *2025 11th International Conference on Automation, Robotics, and Applications (ICARA)*, 2025, pp. 290–299.

[2] Z. M. Kassas, J. Khalife, A. A. Abdallah, and C. Lee, "I am not afraid of the GPS jammer: Resilient navigation via signals of opportunity in GPS-denied environments," *IEEE Aerospace and Electronic Systems Magazine*, vol. 37, no. 7, pp. 4–19, 2022.

[3] A. G. Stove, A. L. Hume, and C. J. Baker, "Low probability of intercept radar strategies," *IEE Proceedings - Radar, Sonar and Navigation*, vol. 151, no. 5, pp. 249–260, 2004.

[4] A. Boukerche, H. A. B. F. Oliveira, E. F. Nakamura, and A. A. F. Loureiro, "Localization systems for wireless sensor networks," *IEEE Wireless Communications*, vol. 14, no. 6, pp. 6–12, 2007.

[5] H. Liu, H. Darabi, P. Banerjee, and J. Liu, "Survey of wireless indoor positioning techniques and systems," *IEEE Transactions on Systems, Man, and Cybernetics, Part C (Applications and Reviews)*, vol. 37, no. 6, pp. 1067–1080, 2007.

[6] P. Zand, J. Romme, J. Govers, F. Pasveer, and G. Dolmans, "A high-accuracy phase-based ranging solution with Bluetooth Low Energy (BLE)," in *2019 IEEE Wireless Communications and Networking Conference (WCNC)*, 2019, pp. 1–8.

[7] Y. Schröder and L. Wolf, "InPhase: Phase-based ranging and localization," *ACM Trans. Sen. Netw.*, vol. 18, no. 2, art. no. 24, Jan. 2022.

[8] N. Patwari, A. O. Hero, M. Perkins, N. S. Correal, and R. J. O'Dea, "Relative location estimation in wireless sensor networks," *IEEE Transactions on Signal Processing*, vol. 51, no. 8, pp. 2137–2148, 2003.

[9] S. Y. Seidel and T. S. Rappaport, "914 MHz path loss prediction models for indoor wireless communications in multifloored buildings," *IEEE*

Transactions on Antennas and Propagation, vol. 40, no. 2, pp. 207–217, 1992.

[10] K. Shamaei, J. Khalife, and Z. M. Kassas, "Exploiting LTE signals for navigation: Theory to implementation," *IEEE Transactions on Wireless Communications*, vol. 17, no. 4, pp. 2173–2189, 2018.

[11] T. S. Rappaport, *Wireless Communications: Principles and Practice*, 2nd ed. USA: Prentice Hall PTR, 2001.

[12] P. Bahl and V. N. Padmanabhan, "RADAR: an in-building RF-based user location and tracking system," in *Proceedings IEEE INFOCOM 2000. Conference on Computer Communications. Nineteenth Annual Joint Conference of the IEEE Computer and Communications Societies (Cat. No.00CH37064)*, vol. 2, 2000, pp. 775–784.

[13] S. Zhou and J. K. Pollard, "Position measurement using Bluetooth," *IEEE Transactions on Consumer Electronics*, vol. 52, no. 2, pp. 555–558, 2006.

[14] Y. T. Chan and K. C. Ho, "A simple and efficient estimator for hyperbolic location," *IEEE Transactions on Signal Processing*, vol. 42, no. 8, pp. 1905–1915, 1994.

[15] S. Kay, "A fast and accurate single frequency estimator," *IEEE Transactions on Acoustics, Speech, and Signal Processing*, vol. 37, no. 12, pp. 1987–1990, 1989.

[16] P. H. Moose, "A technique for orthogonal frequency division multiplexing frequency offset correction," *IEEE Transactions on Communications*, vol. 42, no. 10, pp. 2908–2914, 1994.

[17] T. M. Schmidl and D. C. Cox, "Robust frequency and timing synchronization for OFDM," *IEEE Transactions on Communications*, vol. 45, no. 12, pp. 1613–1621, 1997.

[18] W. Ding and J. Wang, "Precise velocity estimation with a stand-alone GPS receiver," *Journal of Navigation*, vol. 64, no. 2, pp. 311–325, 2011.

[19] Xilinx, "RFSoC-MTS: A PYNQ overlay demonstrating AMD RFSoC multi-tile synchronization," https://github.com/Xilinx/RFSoC-MTS, accessed: 2026-06-10.

[20] M. Székely, "RFSoC-based passive distance and relative radial velocity estimation," https://github.com/szekelymilan/rfsoc-passive-distance-velocity.